International Journal of Automotive Technology, Vol. 14, No. 4, pp. 569–577 (2013)
DOI 10.1007/s12239–013–0061–8

pISSN 1229–9138/ eISSN 1976–3832

HEAT TRANSFER ENHANCEMENT ON VENTILATED BRAKE DISK WITH BLADE INCLINATION ANGLE VARIATION

K. M. MUNISAMY*, N. H. SHUAIB, M. Z. YUSOFF and S. K. THANGARAJU

College of Engineering, Universiti Tenaga Nasional, Jalan IKRAM-UNITEN, Kajang 43009, Malaysia

(Received 25 July 2011; Revised 27 August 2012; Accepted 17 January 2013)

ABSTRACT–Ventilated brake disk is the state of the art technology in automobile braking system. It is well known that the braking capability of brake disk is affected by the rate at which heat is dissipated through forced convection. The rapid increase and decrease of the brake disk temperature could lead to catastrophic failure of the brake disk due to high thermal stress. The objective of the current study is to investigate the potential heat transfer enhancements in ventilated brake disk by varying the geometrical parameters of the blades inside the flow passage. This is done through comparisons of non-dimensional properties for flow and heat transfer in different blade configurations of the ventilated brake disk. The straight blade configuration is used as a baseline reference against the angled blades. The investigations are performed by using both experimental and computational means and the results are compared and discussed. Analysis shows that significant increase in braking performance can be achieved with relatively simple alteration of the ventilated blade angle. The results show a tremendous increase in the heat transfer rate with blade inclination angle configurations as compared to conventional straight blade. The Nusselt number is found to be in a power-law relationship with the Reynolds number. Distinct relationship between laminar and turbulent condition is predicted. An improvement in total convective heat transfer coefficient of 51% was achieved with blade inclination angle of 45° tilting towards clockwise direction.

KEY WORDS : Ventilated brake disk, Heat transfer, CFD

NOMENCLATURE

T_d	: disk temperature(K)
Re	: rotational reynolds number
h_c	: convective heat transfer (W/m^2K)
q_w	: heat flux from wall (W/m^2)
d_o	: outer diameter of the disk (m)
T_w	: wall temperature (K)
T_∞	: ambient temperature (K)
T_f	: near wall fluid temperature (K)
T^+	: dimensionless near-wall temperature
u^*	: relative velocity (m/s)
Pr	: prandtl number
HT	: heater (Watt)
h_d	: conductive heat transfer (W/m^2)
A_w	: disk wetted convective heat dissipation (m^2)
A_{rad}	: disk are, radiative heat dissipation (m^2)
m_d	: mass of the disk (kg)
Nu	: nusselt number
ω	: rotational speed (rad/s)
v	: air kinematic viscosity (m^2/s)
h_{ave}	: average convective heat transfer (W/m^2)
k	: air thermal conductivity (W/mK)

SUBSCRIPTS

d	: conduction
c	: convection
w	: wall
f	: fluid

1. INTRODUCTION

Braking technology has been improved tremendously since the twentieth century. Throughout the development of the braking technology, the ventilated brake disk is the state of the art technology in automobile braking system. Vehicle designs have been mostly concentrated on vehicle aerodynamics, thus the importance of proper braking systems was always disregarded. The braking system normally consists of the ventilated brake disk, which function as a means of storing energy and dissipating it quickly during braking. The braking process is a very quick process; therefore, the brake disk has to be able to dissipate the energy quickly and efficiently. The brake disc has a fan-like effect, allowing air to flow through it smoothly. The balance between the air flow through brake disk and the convective heat transfer is important and equally complicated to achieve. In this paper it was attempted to improve the heat transfer through changing the inclination angle of the radial blades or vanes. Numerous past

**Corresponding author.* e-mail: kannan@uniten.edu.my

researchers have explored in this area. There are not significant numbers of papers using Computational Fluid Dynamics (CFD). CFD is an effective tool with experimental validation especially for flow visualization and detail understanding of heat transfer trends through inside blade channel. Though CFD is the recent era, it is useful to browse the earlier work in brake disk by Limpert (1975), Sission (1978) and, Newcomp (1979). These early works are mainly dependent on the experimental approach to determine the heat transfer characteristics of the rotor. Sission (1978) has suggested analytical method to predict heat transfer coefficient in ventilated flow and it is validated with experimental apparatus but the analysis has constraints to apply the technique to all ventilated rotor in general.

Richardson and Saunders (1963) also took the lead to research in the rotating disc and the heat transfer trend in varying road speed).

Newcomb (1979) has given a general view about energy dissipation during braking. However, only in certain special case the saving can be worthwhile. Value of the losses in vehicle braking is derived for various types of driving. The flow through ventilated disk brake is obstructed by number of part in wheel installation such as wheel house, tire, brake calipers and others. Kreith and his team have reported heat transfer analytical studies in ventilated disc brake as well (Kreith and Bhoh, 2001; Kreith *et al*., 1959). Krusemann and Schmidt (1995) have studied the effects of the installation components to the amount of air flow and heat transfer coefficient through the disk brake system. They have used a commercial CFD code to conduct the analysis. The disk specimen used is standard radial vane type. The fitting modifications accommodate them to achieve improvement of heat transfer coefficient by 15 percent.

Besides the fitting installation improvement there are attempts directly applied onto the disk rotor itself to improve the heat transfer properties. Kubota *et al*. (2000) from Nissan Motor Co. Ltd. suggested a designing method for a lightweight brake rotor with consideration of weight, shape and each performance requirement factors. Critical performance requirements for a brake disc rotor include heat resistance, high cooling and low vibration. The paper presents a parametric study which conducted on the basis of an analysis of airflow through the ventilation holes as well as a thermal stress analysis and vibration analysis during braking. CFD analysis was done on the ventilated rotor of 150 mm outer radius and flow visualization on a scale down model in a water tank. Three types of ventilated fins are tested. The baseline design is compared with two other designs. One is the alternate-length blade and the other is gourd-shaped design. The gourd-shaped fin design has the highest heat transfer coefficient. Lee *et al*. have reported a semi-empirical algorithm to predict braking performance of passenger cars (Lee *et al*., 2011). The accuracy of the program is improved with input of empirical data for pad compression, hose expansion and the friction coefficient between the pad and rotor.

There are many researchers has developed test rig or experimental apparatus for brake rotor like Bryan *et al*. (2008), Panier *et al*. (2004) and Qi and Day (2006). They have studied many areas such as thermal property, vibration, and wear material property. Mostly the challenge is to measure temperature in rotating rotor. Techniques like optical, and infrared for non-contact and thermocouple and temperature sensitive material coating (paint) for contact measurements are explored. Exposed thermocouple technique developed by Qi (Qi and Day, 2006) is reported as an effective method for measuring interface temperature of a friction pair.

The experimental analysis generally is able to resemble the macro level flow condition of a ventilated disk brake. However, the CFD and PIV approach is worth-while approach to understand the flow structure of the blade or vane channel flow. Johnson in his publication (Johnson *et al*., 2003; McPhee and Johnson, 2008), has reported PIV investigation and analytical calculation with limitation is also done to compare the experimental result. In his recent work (McPhee and Johnson, 2008) the disk specimen studied has about 37 radial fins which diameters are 280 mm. Inlet flow measurement shows significant miss alignment due to the swirling entry of the flow. In the internal flow passage, large separation is found on the suction side surface. The flow rate and heat transfer coefficient is directly proportional to the rotational velocity of the rotor.

Tirovic through his research work has contributed significantly to the railway rotor cooling improvement (Tirovic and Ali, 2001; Galindo-Lopez and Tirovic, 2008; Tirovic, 2009). In his earlier paper (Tirovic and Ali, 2001) he describes the design process of two high-performance, hub-mounted railway disc of difference size and duty. He has shown special interest in CFD simulation in proceeding two papers (Galindo-Lopez and Tirovic, 2008) and (Tirovic, 2009). The paper by Galindo-Lopez and Tirovic (2008) is a study of improving the cooling performance of a radial vane disk brake with alternate smaller vane positioned together with the existing long trapezoidal radial vanes. He has come to conclusion that the smaller vane towards outer diameter yield better result compared all. In the latest publication (Tirovic, 2009), Tirovic has evaluated brake disk system as energy saving system. Both experimental and CFD is performed in his work to investigate and understand the flow structure and heat transfer property. The recent publication by Pevec *et al*. (2012) is reported the application of CFD in early pretesting stage of disk brake design to determine the temperature due to different sequential braking modes.

The flow complexity of ventilated brake disk has motivated the authors in this paper to extend the envelope of study into the blade inclination angle configuration effects. With references to Greilzer *et al*. (2003) and Holman

Table 1. Characteristics of baseline brake disk.

Outer diameter of the disk	255 mm
Flying disk ring/plate inner diameter	145 mm
Single ring/plate thickness	7 mm
Ventilated blade passage height	10 mm
Number of blades	36
Mass	2.81 Kg

(1994) the improvement of the design is conducted. The past reporting on the misalignment of the flow at leading edge of the ventilated blade cultivated the idea to have blade tilted with reference to leading edge in the opposite direction of disk rotation. However, due to the induce flow angle is not of control by designer, the best option is to conduct parametric study on a few angle and to investigate the heat transfer improvement with reduced flow velocity angle with respect to the blade orientation. Experimental analysis is performed to gather flow and temperature data. The detail CFD is done to focus the study onto the velocity profile and heat transfer property for validation. The Nusselt number correlation to the rotational speed is derived for laminar and turbulent condition and compared the performance with the baseline and literature results.

2. DISK GEOMETRY

A commercial-vehicle cast-iron ventilated brake disk is chosen as baseline design. The commercial-car chosen can produce 150bhp@5000rpm. The disk has 36 equally spaced radial blades or vanes as shown in Figure 1. The flow condition is in laminar for the disk rotating speed ranging between 643-1929 rpm ($Re < 2.2\times10^5$) and turbulent between 2089 to 2572 rpm ($Re > 2.2\times10^5$) (Dorfman, 1963). The disk is a non-anticoning design.

The flow characteristics and heat transfer properties are studied theoretically using computational fluid dynamics (CFD) simulations and experimentally using rotating test rig. The disk is rotated in still air corresponding to the respective road speed as in Table 2 for both modeling and experimental investigations. This simplifies the study of flow and convective cooling inside the ventilated blades and it is easily repeated under identical conditions. It is certain that any design that shows cooling characteristics improvement in quiescent air will also be superior in cross flow condition as the real car driving condition.

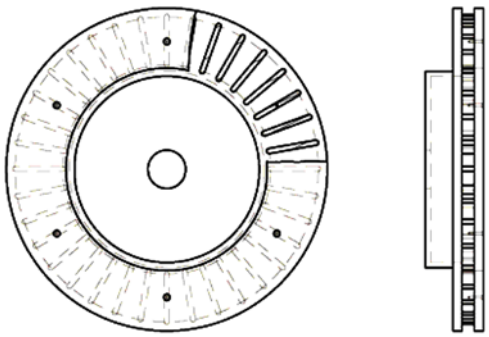

Figure 1. Baseline brake disk.

Table 2. CFD Simulation and Experimental rotational speed configuration.

Road speed (km/h)	Rotational speed (RPM)	Rotational speed (Rad/s)	Rotational Reynolds No.	Flow type
80	643	67	71631	Laminar
100	803	84	89539	Laminar
120	964	101	107455	Laminar
140	1125	117	125354	Laminar
160	1286	135	143262	Laminar
180	1447	151	161171	Laminar
200	1608	168	179078	Laminar
224	1800	188	200506	Laminar
240	1929	202	214934	Laminar
260	2089	218.857	232845	Turbulent
280	2250	235	250757	Turbulent
300	2411	252	268668	Turbulent
320	2572	269	286579	Turbulent

2.1. Ventilated Blade Passage Modifications

The blade modification is done to follow the baseline disk analysis on the flow profile. The specific objective is to eliminate the recirculation area and to tilt the blade in the miss-align angle of the flow (clock-wise direction).

The modifications of the blade configuration are made with the following assumptions:

i. The blade must be position in-between the inner and the outer radius of the baseline design
ii. The thickness remain constant and only the length can be changed to fit the inner and outer radius

The geometries of the new designs with baseline design

Table 3. Blade length against blade inclination angle.

NO	Blade inclination angle (°)	Total length (mm)	Total length percentage increase (%)
1	0	42.00	0
2	15	42.96	2.28
3	25	44.72	6.48
4	30	45.98	9.48
5	35	47.52	13.15
6	45	51.55	22.74

Table 4. Disk design, mass, and wetted area straight blade design.

Disk design	Mass (kg)	Convective wetted area of blade (m^2)
Baseline (0°)	2.18	0.2776
15° Inclination	2.19 (+0.3%)	0.2781 (+0.15%)
30° Inclination	2.21 (+1.4%)	0.2794 (+0.62%
45° Inclination	2.26 (+3.4%)	0.2818 (+1.4%)

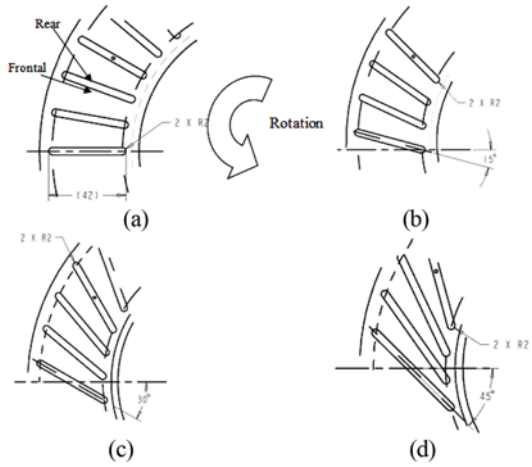

Figure 2. Blade orientation configuration: (a) 0° angle (baseline); (b) 15° angle inclined; (c) 30° angle inclined; (d) 45° angle inclined.

are shown in Figure 2. The inclination angle is the rotational angle in clock-wise direction. The Table 3 lists the blade length and percentage increase. And Table 4 illustrates the mass and wetted area variation for the modified geometries.

3. EXPERIMENTAL APPARATUS

An experimental rig is designed, built and tested the specimen as shown in Figure 3. The experimental rig has ability to measure measurements, such as total flow rate, surface temperature and pressure which collected by Data Acquisition System integrated with the test rig. In the Figure 3, the positions of the measuring devices which placed at the test specimen can be observed. Moreover the brief explanation of the thermocouple location also has been discussed in Table 5. There are Pt-type, K-type and infrared type thermocouples involved in the measurements of temperature. The gas flow meter is used to measure the flow rate. A disk brake casing is designed specifically for the current specimen size with 255 mm outer diameter. The design shows the custom-made Aluminum material casing that guides the outflow radially out and in flow axially directed in through the center of the brake disk with almost zero leakage. The ventilated brake disk of 255 mm diameter

Table 5. Position of thermocouple.

ID	Thermocouple	Location
A	Pt1	R = 125 mm
B	Pt2	R = 110 mm
C	Pt3	R = 95 mm
D	Pt4	R = 125 mm
E	Pt5	R = 110 mm
F	Pt6	R = 95 mm
G	Pt7	Inlet, R = 60 mm
H	Pt8	Outlet, R = 130 mm
I	K1	Ambient

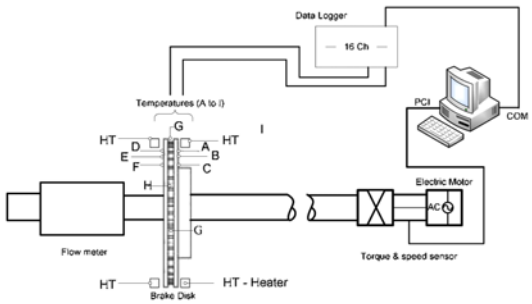

Figure 3. Ventilated brake disk experimental rig.

is fitted with only 1mm clearance between rotating disk and the casing. The tube around the casing is to measure the outlet static pressure. Each of the measuring equipment has systematic error which contributes to the Nusselt number (Nu) calculation and the error of the Nu is estimated to be within 1.02 %.

4. COMPUTATIONAL MODEL DEVELOPMENT

4.1. CFD Disk Model

In CFD the ventilated disk brake are modeled in two flow-through segments of 10° each. The computational model constructed in GAMBIT. The models are solved using ANSYS-FLUENT proprietary software package. Figure 4 shows the model employs periodic boundary conditions on the segmented side. The disk surface considered to be heated at T_d = 100°C. The ambient air is assumed at 25°C. The inlet boundary condition is set to be velocity inlet and the outlet is as pressure outlet. The boundary condition is input from experimental analysis data for respective rotational speed. The rotating frame is set the disk domain and the rotational speed in Rad/s is used for simulating rotational motion as in Table 2. This is done to ensure the ventilated disk brake surface is kept stationary and yet the rotational kinematic effect of centrifugal and Coriolis accelerations are included in the motion equations to avoid transient solution. The computational model constructed in GAMBIT for the two flow channels consist of about 2.5

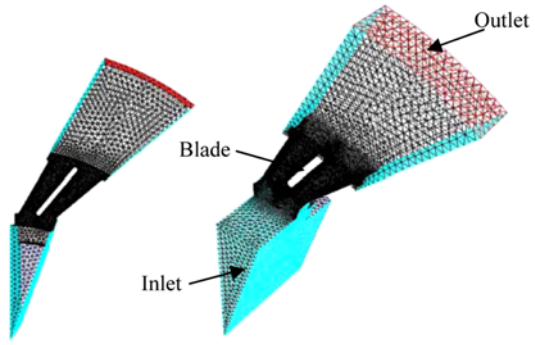

Figure 4. Meshed computational domain in GAMBIT.

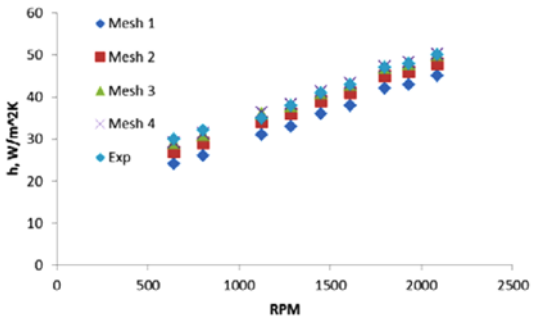

Figure 5. Heat transfer coefficient result against all mesh configurations.

million hexahedral, tetrahedral, and pyramid cells. The boundary layer near the wall is captured using cell height of 0.1 mm and followed by inflation ratio of 1.2. The mesh is selected after mesh dependency study is done comparing to the experimental data which has error around less than 1%.

Convective heat transfer coefficients are calculated using the unperturbed air temperature T_∞. The flow condition is in laminar for the disk rotating speed range form 643-1929 rpm ($Re_\varepsilon < 2.2\times10^5$) (Dorfman, 1963).

4.2. Convective Heat Transfer Calculation

Flow and heat transfer modelling near wall is carried out with assistance of CFD software using speed and temperature logarithmic-law wall functions. In order to have accurate results, a fine grid near walls is required so that energy transfer to the core of the fluid is captured well. The heat transfer is calculated as

$$h_c = q_w(T_w - T_\infty)^{-1} \tag{1}$$

The heat flux form the wall, q_w, is modelled following the log-law wall function, using relative velocity u^*, dimensionless near-wall turbulent temperature T^+, a specified wall temperature condition T_w and a near-wall fluid temperature T_f.

$$q_w = \frac{\rho c_p u^*}{T^+}(T_w - T_f) \tag{2}$$

Dry air fluid properties were adopted. The T^+ can be defined as

$$T^+ = Pry^+ e^{-r} + [2.12 ln y^* + \beta] e^{-\Gamma=1} \tag{3}$$

$$y^+ = \frac{u^* \Delta y}{v} \tag{4}$$

The functions y^*, β, and Γ are empirical functions depending upon y^+, geometry, and Prandtl number *(Pr)* and Δy accounts for the distance from the first to the second nodes. The solver treatment of the near-wall grid node allows Δy to be redefined by dividing the space between the first and second nodes by 4 (Kader, 1981).

4.3. Mesh Dependency Investigation

The mesh dependency analysis is done on 4 configurations of computational grid on the baseline design. Before examining the mesh developed in detail, it is worth looking at the quantity and time taken for each mesh configurations as listed in Table 6 below. The Figure 5 illustrates the 3-dimensional computational domain which consists of 3 separate volume or computational blocks. The inlet side (bottom volume) and the outlet side (top volume) will follow the blade side mesh concentration and lease interest of the author. Thus, the Table 6 only compares the blade volume mesh quantity which is also in the rotating frame of reference. Obviously the Mesh 1, 2, 3, and 4 has increasing blade volume mesh quantity. The Mesh 4 is finest mesh of all. The mesh quantity is obtained using size function available in GAMBIT mesh generating software. The increasing mesh number has significant impact onto the computational time on the 16 core High Performance Computing (HPC) machine by Silicon Graphic Incorporated (SGI) that is installed in the department. The computational time is almost linear proportional to the number of mesh. The coarsest mesh has computation time of 65 min to the finest with 8 times increment in computation time.

The results of the heat transfer coefficients are plotted against the experimental data in Figure 5.

As expected the *Mesh 1* has the lowest heat transfer coefficient values of all mesh configurations for all rotational speeds in Figure 5. The *Mesh 2*, *Mesh 3*, and *Mesh 4* predicts closely to each other. The difference is less than 1% for Mesh 4 against experimental data. Ideally author aims to obtain the CFD result in shortest computation time with highest possible level of confidence. However, from the results presented on Figure 5 the Mesh 4 will be the ideal mesh configuration which has lowest error with experimental.

5. HEAT TANSFER ANALYSIS

The detail analysis is vital to make clear the flow behaviour which then influenced the heat transfer property of the brake disk designs. Firstly, the mass flow rate against Reynolds number is plotted in Figure 6. The trend linear and the mass flow is increasing with blade angle inclination

Table 7. Mass flow rate at 1125 rpm.

Disk design	Mass flow rate (g/s)	Relative difference (%)
Baseline	10.13	-
15° brake disk	10.55	+4.1
30° brake disk	12.46	+23
45° brake disk	14.27	+41

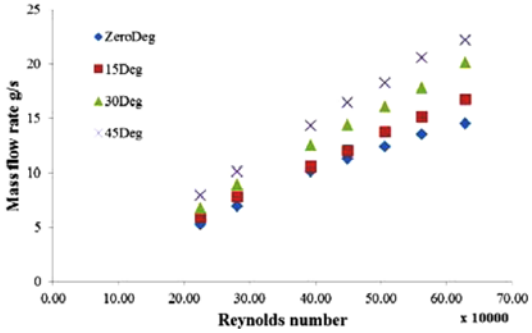

Figure 6. Experimental Mass flow measurement through for baseline (0), 15, 30, and 45 inclination angle of straight blade brake disks.

angle. The velocity contour distributions are shown in Figure 7 for selected rotational speed of 1125 rpm. The 15° brake disk has recorded velocity of around 18 m/s over the frontal area. The 30° brake disk has a slight increment around 19 m/s, and followed by 45° brake disk at 25 m/s. The contour plot also predicts an interesting pattern in terms of the velocity concentration in the frontal and rear side. It is important to recall that the velocity is concentrated towards rear side of the flow passage in baseline design. The trend is still similar for 15° however the frontal side lower velocity region has reduced. The 30° and 45° blade designs velocity distribution show that the lower flow region has moved from rear to frontal side of the blade.

The temperature distributions at the mid-flow plane for all straight blade designs are presented in Figure 8. The temperature follows similar trend as the air velocity contour. The rear side temperature is lower than the frontal side of the flow passage for 15° blade design. The reddish color is for the highest value which is concentrated at rear side of the ventilated blade. For 30° disk brake temperature distribution, the higher temperature is visible at frontal and rear side as in the Figure 8. The 45° blade design shows that the high temperature region is concentrated at the frontal side. The temperature distribution is very much follows the trend of velocity distribution for all straight blade configurations. The high temperature shows poor heat dissipation to the convective air flow.

The heat transfer coefficient is plotted in Figure 9 for all 4 disk brake configurations. Each experimental disk data is compared with CFD and shows a close correlation. The

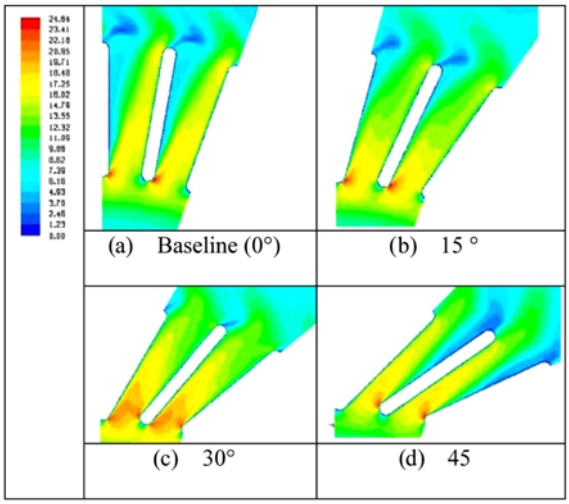

Figure 7. Velocity contour plot for inclined brake disk design at 1125 rpm.

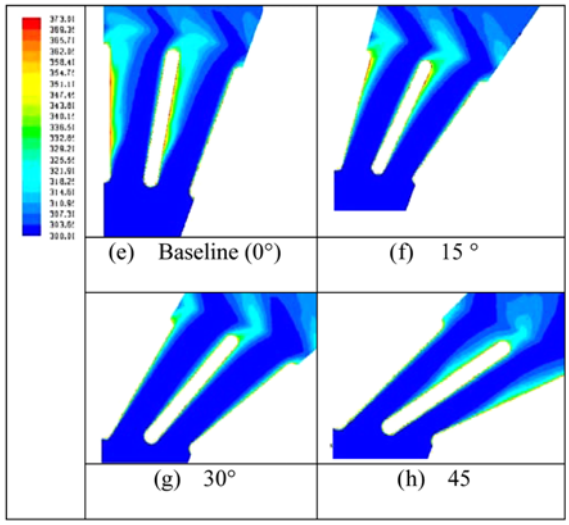

Figure 8. Temperature contour plot for inclined brake disk design at 1125 rpm.

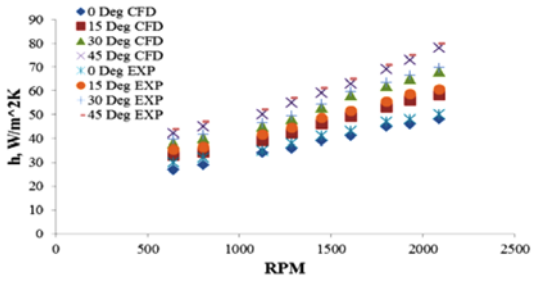

Figure 9. Validation of CFD modeling with experimental of heat transfer coefficient for laminar flow condition for Incline bladed disk brake.

heat transfer performance is in accordance with mass flow data. The baseline having the lowest heat transfer

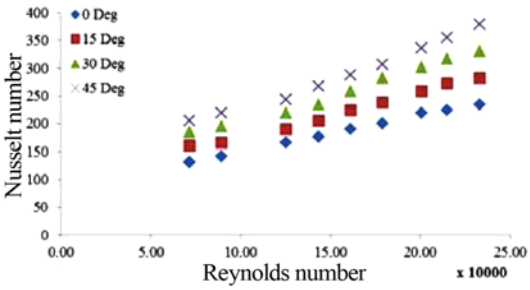

Figure 10. CFD Average Nusselt number for 0, 15, 30, and 45 inclination angle of brake disk for laminar flow region.

performance and in order follows by 15°, 30° and 45° has the highest performance.

Table 7 illustrates the convective cooling characteristics and mass flow comparison for all straight blade configurations at 1125 rpm rotational speed. The 45° disk brake has about 41% increment in mass flow rate compared to the baseline disk. The cooling performance has increased to 37% for 30° blade and 51% for 45° blade configuration disk brake from the baseline design. Similar trend of heat transfer coefficient increment is noticed for all the rotational speed. The relationship of the heat transfer and the rotational speed for laminar and turbulent is found to be different as highlighted in the literatures.

6. DISCUSSION

The heat transfer has significant improvement with inclination angle of ventilated blade configuration. The improvement of average Nusselt number (disk radius based) is calculated for 15°, 30° and 45° and presented in Figure 10 and Figure 11 for laminar and turbulent flow condition. Obviously the 45° brake disk shows the most superior cooling property compared to all brake disk specimen. The baseline design has the worst cooling characteristics of all.

The relationship between the Nusselt number and the Rotational Reynolds number is observed for all the inclined straight blade designs.

The following relationship established for the Nusselt number result presented in Figure 10 for laminar flow condition.

For baseline disk:

$$Nu = 0.455\left(\frac{\omega d_o^2}{4v}\right)^{0.5039} \quad (5)$$

For 15° disk:

$$Nu = 0.5063\left(\frac{\omega d_o^2}{4v}\right)^{0.5094} \quad (6)$$

For 30° disk:

$$Nu = 0.5339\left(\frac{\omega d_o^2}{4v}\right)^{0.5176} \quad (7)$$

For 45° disk:

$$Nu = 0.5372\left(\frac{\omega d_o^2}{4v}\right)^{0.5262} \quad (8)$$

The laminar relationship listed above has two important parameters to be noticed. The coefficient constant in front of the Reynolds number and the power-law value. The coefficient constant is predicted to vary from 0.45 to 0.53 for all designs. The power of power-law relationship for Nusselt number is increasing with increasing blade inclination angle between the ranging from 0.50 to 0.53. The improvement at 1125 rpm is shown in the Table 8.

The following relationship established for the Nusselt number result presented in Figure 11 for turbulent flow condition:

For baseline disk:

$$Nu = 0.0138\left(\frac{\omega d_o^2}{4v}\right)^{0.7918} \quad (9)$$

For 15° disk:

$$Nu = 0.0125\left(\frac{\omega d_o^2}{4r}\right)^{0.8144} \quad (10)$$

For 30° disk:

$$Nu = 0.0139\left(\frac{\omega d_o^2}{4v}\right)^{0.9172} \quad (11)$$

For 45° disk:

$$Nu = 0.0137\left(\frac{\omega d_o^2}{4v}\right)^{0.8286} \quad (12)$$

The power of power-law relationship for Nusselt number is increasing with increasing blade inclination angle between

Table 6. Meshing configurations for baseline disk brake.

Mesh configuration	Size function setting - blade volume only		Total mesh quantity	Convergence time **(min)** in 16 core HPC machine	
	Start size	Growth rate	(cells)	(Single speed configuration)	(13 speeds configurations)
Mesh 1	1	1.2	95,793	5	65
Mesh 2	0.75	1.2	195,766	10	130
Mesh 3	0.5	1.2	413,096	20	260
Mesh 4	0.4	1.2	740,661	40	520

Table 8. Average convective cooling characteristics at 1125 rpm for straight blade designs.

Disk design	h_{avr} (W/m^{2}K) (CFD)	Relative difference (%)	Mass flow rate (g/s)	Relative difference (%)
Baseline	34	-	10.13	-
15° Brake disk	39	+16	10.55	+4.1
30° Brake disk	45	+37	12.46	+23
45° Brake disk	50	+51	14.27	+41

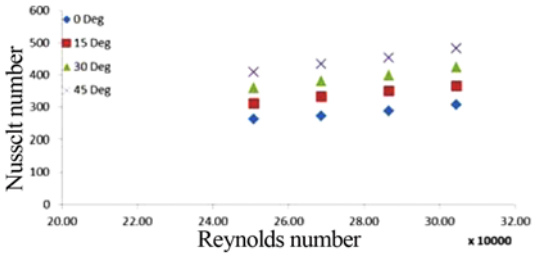

Figure 11. CFD Average Nusselt number for 0, 15, 30, and 45 inclination angle of brake disk for turbulent flow region.

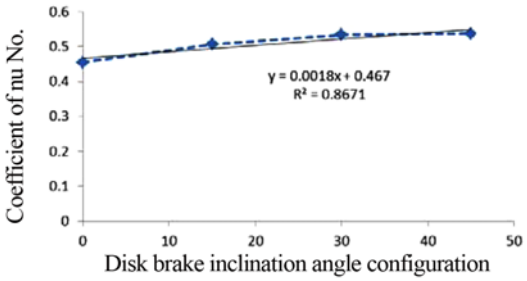

Figure 12. Relationship between the coefficient of Nusselt number against Disk brake blade angle configuration.

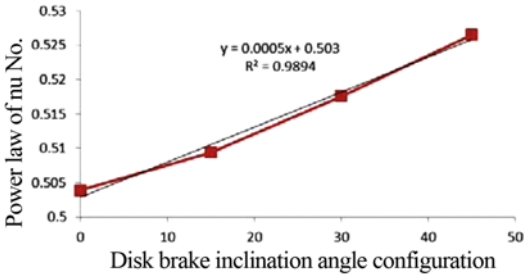

Figure 13. Relationship between the power law of Nusselt number against Disk brake blade angle configuration.

the ranging from 0.79 to 0.83.The coefficient constant is predicted ranging between 0.013 to 0.014 for all design.

The laminar power-law has average value of 0.5 and the turbulent power-law is at 0.8 which is very similar to the literatures. However, a small increment of the power-law with the magnitude of 0.01 in both cases has significant effect in the heat transfer performance and it plays the dominant impact as compared to the coefficient constant. The trend of the coefficient and power law against blade inclination angle can be seen in Figure 12 and Figure 13 respectively. Both has linear relationship. However, the power law has steeper slope than the coefficient and that's valuable information for designers to vary the blade inclination angle for the desired heat transfer.

7. CONCLUSION

Firstly, the conventional brake disk which is addressed as baseline disk brake design is improved with blade inclination effect to streamline the flow profile inside the flow passage which was highly influence by the induced rotational flow. Focusing on the ventilated blade passage air flow pattern made the blade modification a worth-while effort to improve the heat dissipation rate. Angle inclination has made the flow pattern re-aligned and the induced mass flow to increase. Recirculation was also eliminated completely in 30° blade design. Recirculation and air stagnation are major culprits to improve convective cooling performance.

The modification has improved heat dissipation about 32% for 30° with mass flow increment of 23%. The extreme trial of ventilated blade angle at 45° configuration has yielded a tremendous improvement of 47% heat transfer coefficient which is a direct reflect of air flow realignment. The relationship shows the exponential value increasing with increasing inclination angle. The exponential is more dominant than the coefficient constant of the Nusselt number relationship against Reynolds number.

REFERENCE

Bryant, D., Fieldhouse, J., Crampton, A. and Talbot, C. (2008). Thermal brake judder investigations using a high speed dynamometer. *SAE Paper No.* 2008-01-0818, 14–17.

Dorfman, L. (1963). *Hydrodynamic Resistance and the Heat Loss of Ratating Solids.* Oliver and Boyd. Edinburgh.

Galindo-Lopez, C. and Tirovic, M. (2008). Understanding and improving the convective cooling of the brake discs with radial vanes. *Proc. Instn. Mech. Engrs.*, *Part D*, *J. Automobile Engineering*, **222**, 1211–1229.

Greilzer, E., Tan, C. and Graf, M. (2003). *Internal Flow, Concepts and Applications.* Cambridge University Press. Cambridge. UK.

Holman, J. P. (1994). *Experimentation Methods for*

Engineers. McGraw- Hill. New York. 47.

Johnson, D. A., Sperandei, B. A. and Gilbert, R. (2003). Analysis of the flow through a vented automotive brake rotor. *ASME J. Fluids Engineering*, **125**, 979–986.

Kader, B. (1981). Temperature and concentration profiles in fully turbulent boundary layers. *Int. J. Heat Mass Transfer* **24**, **9**, 1541–1544.

Kreith, F. and Bohn, M. (2001). *Principles of Heat Transfer.* Brooks/Cole Thomson Learning. New York.

Kreith, F., Taylor, J. and Chong, J. (1959). Heat and mass transfer from a rotating disk. *Trans*. *ASME J. Heat Transfer*, **81**, 95–105.

Krusemann, R. and Schmidt, G. (1995). Analysis and optimization of disk brake cooling via computational fluid dynamics. *SAE Paper No*. 950791.

Kubota, M., Hamab, T. and Nakazono, Y. (2000). Development of a light weight brake disc rotor: A design approach for achieving an optimum thermal, vibration and weight balance. *JSAE*, **21**, 349–355.

Lee, C. H., Lee, J.-M., Choi, M.-S., Kim, C.-K. and Koh, E.-B. (2011). Development of a semi-empirical program for predicting the braking performance of a passenger vehicle. *Int. J. Automotive Technology* **12**, **2**, 193–198.

Limpert, R. (1975). The thermal performance of automotive disc brakes. *SAE Paper No*. 750873.

McPhee, A. and Johnson, D. (2008). Experimental heat trasnfer and flow analysis of a ventied brake rotor. *Int. J. Thermal Sciences*, **47**, 458–467.

Newcomb, T. (1980). Energy dissipated during braking. *Proc. Wear*, 401–407.

Panier, S., Dufrenoy, P. and Weichert, D. (2004). An experimental investigation of hot spots in railway disc brakes. *Proc. Wear*, **256**, 764–773.

Pevec, M., Potrc, I., Bombek, G. and Vranesevic, D. (2012). Prediction of the cooling factors of a vehicle brake disc and its influence on the results of a thermal numerical simulation. *Int. J. Automotive Technology* **13**, **5**, 725–733.

Qi, H. and Day, A. (2006). Investigation of disc/pad interface temperature in friction braking. *Proc*. *Wear*, **262**, 505–513.

Richardson, P. and Saunders, O. (1963). Studies of flow and heat transfer associated with a rotaing disc. *J. Mechanical Engineering Science* **5**, **4**, 336–342.

Sission, A. (1978). Thermal analysis of vented brake rotors. *SAE Paper No*. 780352.

Tirovic, M. (2009). Energy thrift and improved performance achevied through novel railway brake discs. *Applied Energy*, **86**, 317–324.

Tirovic, M. and Ali, G. (2001). Design synthesis of non-symmetrically loaded high-performance disc brakes part 1. *Proc. IMechE Part F*, **215**, 101–109.